

CPB

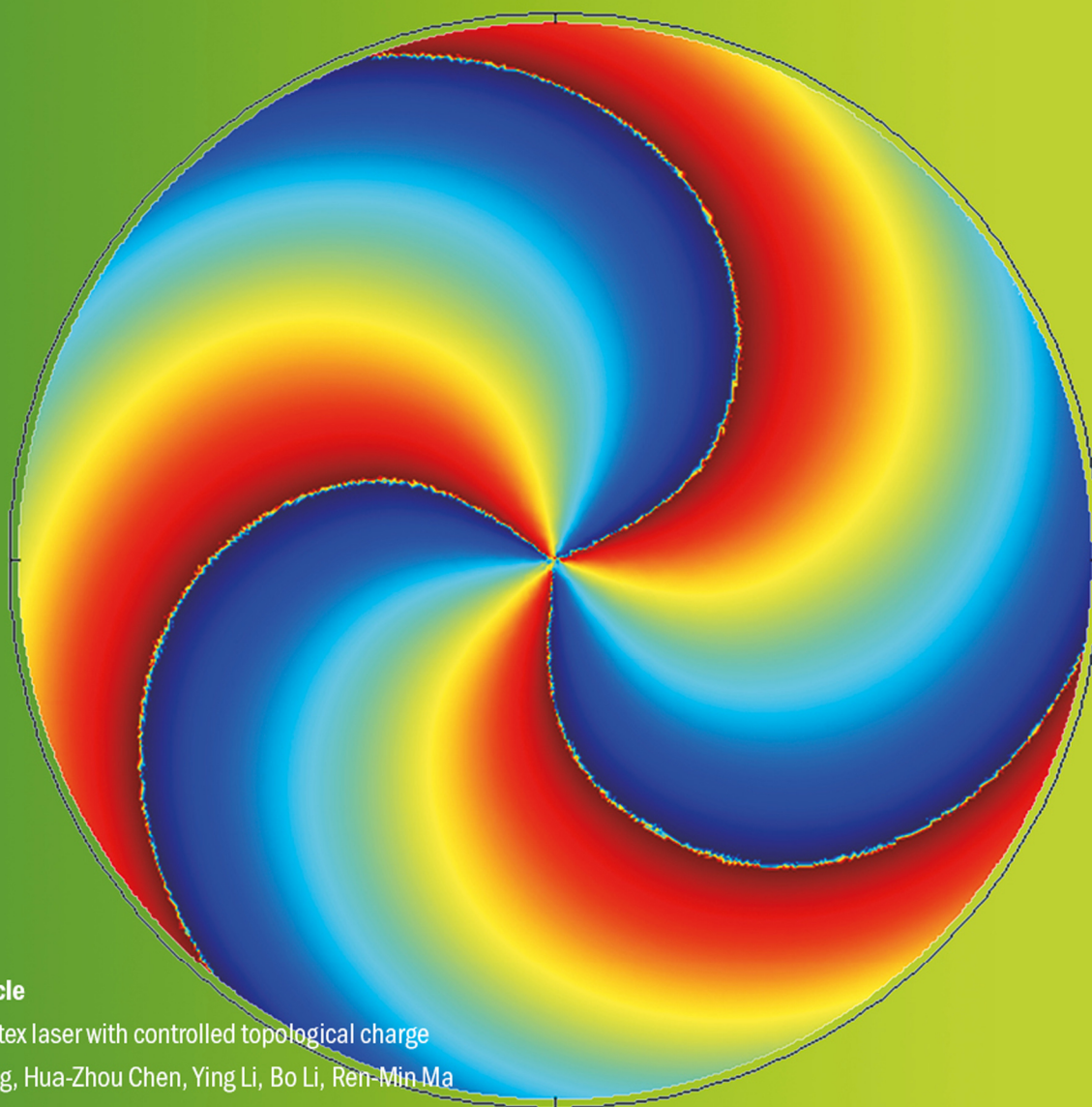
Chinese Physics B

SPECIAL TOPIC

• Acoustics

A Series Journal of the Chinese Physical Society Distributed by IOP Publishing

iopscience.org/cpb | cpb.iphy.ac.cn



Featured Article

Microscale vortex laser with controlled topological charge

Xing-Yuan Wang, Hua-Zhou Chen, Ying Li, Bo Li, Ren-Min Ma

doi: 10.1088/1674-1056/25/12/124211

Chinese Physics B

(First published in 1992)

Published monthly in hard copy by the Chinese Physical Society and online by IOP Publishing, Temple Circus, Temple Way, Bristol BS1 6HG, UK

Institutional subscription information: 2015 volume

For all countries, except the United States, Canada and Central and South America, the subscription rate per annual volume is UK£974 (electronic only) or UK£1063 (print + electronic).

Delivery is by air-speeded mail from the United Kingdom.

Orders to:

Journals Subscription Fulfilment, IOP Publishing, Temple Circus, Temple Way, Bristol BS1 6HG, UK
For the United States, Canada and Central and South America, the subscription rate per annual volume is US\$1925 (electronic only) or US\$2100 (print + electronic). Delivery is by transatlantic airfreight and onward mailing.

Orders to: IOP Publishing, P. O. Box 320, Congers, NY 10920-0320, USA

© 2015 Chinese Physical Society and IOP Publishing Ltd

All rights reserved. No part of this publication may be reproduced, stored in a retrieval system, or transmitted in any form or by any means, electronic, mechanical, photocopying, recording or otherwise, without the prior written permission of the copyright owner.

Supported by the China Association for Science and Technology and Chinese Academy of Sciences

Editorial Office: Institute of Physics, Chinese Academy of Sciences, P. O. Box 603, Beijing 100190, China

Tel: (86-10) 82649026 or 82649519, Fax: (86-10) 82649027, E-mail: cpb@aphy.iphy.ac.cn

主管单位: 中国科学院

国际统一刊号: ISSN 1674-1056

主办单位: 中国物理学会和中国科学院物理研究所

国内统一刊号: CN 11-5639/O4

主 编: 欧阳钟灿

编辑部地址: 北京 中关村 中国科学院物理研究所内

出 版: 中国物理学会

通 讯 地 址: 100190 北京 603 信箱

印刷装订: 北京科信印刷有限公司

电 话: (010) 82649026, 82649519

编 辑: Chinese Physics B 编辑部

传 真: (010) 82649027

国内发行: Chinese Physics B 出版发行部

“Chinese Physics B”网址:

国外发行: IOP Publishing Ltd

<http://cpb.iphy.ac.cn> (编辑部)

发行范围: 公开发行

<http://iopscience.iop.org/cpb> (IOPP)

Published by the Chinese Physical Society

顾问 Advisory Board

| | | |
|-----|----------------------------------|--|
| 陈佳洱 | 教授, 院士 北京大学物理学院, 北京 100871 | Prof. Academician Chen Jia-Er School of Physics, Peking University, Beijing 100871, China |
| 冯 端 | 教授, 院士 南京大学物理系, 南京 210093 | Prof. Academician Feng Duan Department of Physics, Nanjing University, Nanjing 210093, China |
| 李政道 | 教授, 院士 | Prof. Academician T. D. Lee Department of Physics, Columbia University, New York, NY 10027, USA |
| 李荫远 | 研究员, 院士 中国科学院物理研究所, 北京 100190 | Prof. Academician Li Yin-Yuan Institute of Physics, Chinese Academy of Sciences, Beijing 100190, China |
| 丁肇中 | 教授, 院士 | Prof. Academician Samuel C. C. Ting LEP3, CERN, CH-1211, Geneva 23, Switzerland |
| 杨振宁 | 教授, 院士 | Prof. Academician C. N. Yang Institute for Theoretical Physics, State University of New York, USA |
| 杨福家 | 教授, 院士 复旦大学物理二系, 上海 200433 | Prof. Academician Yang Fu-Jia Department of Nuclear Physics, Fudan University, Shanghai 200433, China |
| 周光召 | 研究员, 院士 中国科学技术协会, 北京 100863 | Prof. Academician Zhou Guang-Zhao (Chou Kuang-Chao) China Association for Science and Technology, Beijing 100863, China |
| 王乃彦 | 研究员, 院士 中国原子能科学研究院, 北京 102413 | Prof. Academician Wang Nai-Yan China Institute of Atomic Energy, Beijing 102413, China |
| 梁敬魁 | 研究员, 院士 中国科学院物理研究所, 北京 100190 | Prof. Academician Liang Jing-Kui Institute of Physics, Chinese Academy of Sciences, Beijing 100190, China |

2012-2015

主 编 Editor-in-Chief

欧阳钟灿 研究员, 院士
中国科学院理论物理研究所,
北京 100190

Prof. Academician Ouyang Zhong-Can
Institute of Theoretical Physics, Chinese Academy of Sciences,
Beijing 100190, China

副主编 Associate Editors

赵忠贤 研究员, 院士
中国科学院物理研究所, 北京 100190

Prof. Academician Zhao Zhong-Xian
Institute of Physics, Chinese Academy of Sciences, Beijing 100190, China

杨国桢 研究员, 院士
中国科学院物理研究所, 北京 100190

Prof. Academician Yang Guo-Zhen
Institute of Physics, Chinese Academy of Sciences, Beijing 100190, China

张 杰 研究员, 院士
上海交通大学物理与天文系,
上海 200240

Prof. Academician Zhang Jie
Department of Physics and Astronomy, Shanghai Jiao Tong University,
Shanghai 200240, China

邢定钰 教授, 院士
南京大学物理学院, 南京 210093
沈保根 研究员, 院士
中国科学院物理研究所, 北京 100190
龚旗煌 教授, 院士
北京大学物理学院, 北京 100871
沈平 教授
香港科技大学物理学系, 香港九龍

编辑委员 Editorial Board

2011–2016

Prof. F. R. de Boer

Prof. H. F. Braun

陈东敏 教授

冯世平 教授
北京师范大学物理系, 北京 100875

高鸿钧 研究员, 院士
中国科学院物理研究所, 北京 100190

顾长志 研究员
中国科学院物理研究所, 北京 100190

胡岗 教授
北京师范大学物理系, 北京 100875

侯建国 教授, 院士
中国科学技术大学中国科学院结构分析
重点实验室, 合肥 230026

李方华 研究员, 院士
中国科学院物理研究所, 北京 100190

闵乃本 教授, 院士
南京大学物理系, 南京 210093

聂玉昕 研究员
中国科学院物理研究所, 北京 100190

潘建伟 教授, 院士
中国科学技术大学近代物理系,
合肥 230026

沈志勋 教授

苏肇冰 研究员, 院士
中国科学院理论物理研究所,
北京 100190

孙昌璞 研究员, 院士
中国工程物理研究院北京计算科学
研究中心, 北京 100094

王恩哥 研究员, 院士
北京大学物理学院, 北京 100871

夏建白 研究员, 院士
中国科学院半导体研究所,
北京 100083

向涛 研究员, 院士
中国科学院理论物理研究所,
北京 100190

谢心澄 教授
北京大学物理学院, 北京 100871

詹文龙 研究员, 院士
中国科学院, 北京 100864

朱邦芬 教授, 院士
清华大学物理系, 北京 100084

2013–2018

Prof. Antonio H. Castro Neto

Prof. Chia-Ling Chien

Prof. David Andelman

Prof. Masao Doi

Prof. Michiyoshi Tanaka

Prof. Werner A. Hofer

丁军 教授

贺贤士 研究员, 院士
北京应用物理与计算数学研究所,
北京 100088

金晓峰 教授
复旦大学物理系, 上海 200433

Prof. Academician Xing Ding-Yu
School of Physics, Nanjing University, Nanjing 210093, China

Prof. Academician Shen Bao-Gen
Institute of Physics, Chinese Academy of Sciences, Beijing 100190, China

Prof. Academician Gong Qi-Huang
School of Physics, Peking University, Beijing 100871, China

Prof. Sheng Ping
Department of Physics, The Hong Kong University of Science and Technology,
Kowloon, Hong Kong, China

van der Waals-Zeeman Institute der Universiteit van Amsterdam
Valckenierstraat 65, 1018 XE Amsterdam, **The Netherlands**
Physikalisches Institut, Universität Bayreuth, D-95440 Bayreuth, **Germany**

Prof. Chen Dong-Min
Rowland Institute for Science, Harvard University, **USA**

Prof. Feng Shi-Ping
Department of Physics, Beijing Normal University, Beijing 100875, China

Prof. Academician Gao Hong-Jun
Institute of Physics, Chinese Academy of Sciences, Beijing 100190, China

Prof. Gu Chang-Zhi
Institute of Physics, Chinese Academy of Sciences, Beijing 100190, China

Prof. Hu Gang
Department of Physics, Beijing Normal University, Beijing 100875, China

Prof. Academician Hou Jian-Guo
Structure Research Laboratory, University of Science and Technology of
China, Hefei 230026, China

Prof. Academician Li Fang-Hua
Institute of Physics, Chinese Academy of Sciences, Beijing 100190, China

Prof. Academician Min Nai-Ben
Department of Physics, Nanjing University, Nanjing 210093, China

Prof. Nie Yu-Xin
Institute of Physics, Chinese Academy of Sciences, Beijing 100190, China

Prof. Academician Pan Jian-Wei
Department of Modern Physics, University of Science and Technology of
China, Hefei 230026, China

Prof. Shen Zhi-Xun
Stanford University, Stanford, CA 94305–4045, **USA**

Prof. Academician Su Zhao-Bing
Institute of Theoretical Physics, Chinese Academy of Sciences,
Beijing 100190, China

Prof. Academician Sun Chang-Pu
Beijing Computational Science Research Center, China Academy of
Engineering Physics, Beijing 100094, China

Prof. Academician Wang En-Ge
School of Physics, Peking University, Beijing 100871, China

Prof. Academician Xia Jian-Bai
Institute of Semiconductors, Chinese Academy of Sciences,
Beijing 100083, China

Prof. Academician Xiang Tao
Institute of Theoretical Physics, Chinese Academy of Sciences,
Beijing 100190, China

Prof. Xie Xin-Cheng
School of Physics, Peking University, Beijing 100871, China

Prof. Academician Zhan Wen-Long
Chinese Academy of Sciences, Beijing 100864, China

Prof. Academician Zhu Bang-Fen
Department of Physics, Tsinghua University, Beijing 100084, China

Physics Department, Faculty of Science, National University of Singapore,
Singapore 117546, **Singapore**

Department of Physics and Astronomy, The Johns Hopkins University,
Baltimore, MD 21218, **USA**

School of Physics and Astronomy, Tel Aviv University, Tel Aviv 69978,
Israel

Toyota Physical and Chemical Research Institute, Yokomichi, Nagakute,
Aichi 480-1192, **Japan**

Research Institute for Scientific Measurements, Tohoku University, Katahira
2-1-1, Aoba-ku 980, Sendai, **Japan**

Stephenson Institute for Renewable Energy, The University of Liverpool,
Liverpool L69 3BX, **UK**

Prof. Ding Jun
Department of Materials Science & Engineering, National University of
Singapore, Singapore 117576, **Singapore**

Prof. Academician He Xian-Tu
Institute of Applied Physics and Computational Mathematics, Beijing 100088,
China

Prof. Jin Xiao-Feng
Department of Physics, Fudan University, Shanghai 200433, China

李儒新 研究员
中国科学院上海光学精密机械研究所,
上海 201800

吕力 研究员
中国科学院物理研究所, 北京 100190

李晓光 教授
中国科学技术大学物理系, 合肥 230026

沈元壤 教授

王亚愚 教授
清华大学物理系, 北京 100084

王玉鹏 研究员
中国科学院物理研究所, 北京 100190

王肇中 教授

闻海虎 教授
南京大学物理学院系, 南京 210093

徐至展 研究员, 院士
中国科学院上海光学精密机械研究所,
上海 201800

许岑珂 助理教授

薛其坤 教授, 院士
清华大学物理系, 北京 100084

叶军 教授

张振宇 教授

Prof. Li Ru-Xin
Shanghai Institute of Optics and Fine Mechanics, Chinese Academy of Sciences, Shanghai 201800, China

Prof. Lü Li
Institute of Physics, Chinese Academy of Sciences, Beijing 100190, China

Prof. Li Xiao-Guang
Department of Physics, University of Science and Technology of China, Hefei 230026, China

Prof. Shen Yuan-Rang
Lawrence Berkeley National Laboratory, Berkeley, CA 94720, USA

Prof. Wang Ya-Yu
Department of Physics, Tsinghua University, Beijing 100084, China

Prof. Wang Yu-Peng
Institute of Physics, Chinese Academy of Sciences, Beijing 100190, China

Prof. Wang Zhao-Zhong
Laboratory for Photonics and Nanostructures(LPN) CNRS-UPR20, Route de Nozay, 91460 Marcoussis, France

Prof. Wen Hai-Hu
School of Physics, Nanjing University, Nanjing 210093, China

Prof. Academician Xu Zhi-Zhan
Shanghai Institute of Optics and Fine Mechanics, Chinese Academy of Sciences, Shanghai 201800, China

Assist. Prof. Xu Cen-Ke
Department of Physics, University of California, Santa Barbara, CA 93106, USA

Prof. Academician Xue Qi-Kun
Department of Physics, Tsinghua University, Beijing 100084, China

Prof. Ye Jun
Department of Physics, University of Colorado, Boulder, Colorado 80309-0440, USA

Prof. Z. Y. Zhang
Oak Ridge National Laboratory, Oak Ridge, TN 37831-6032, USA

2015-2020

Prof. J. Y. Rhee
Prof. Robert J. Joynt

程建春 教授
南京大学物理学院, 南京 210093

戴希 研究员
中国科学院物理研究所, 北京 100190

郭光灿 教授, 院士
中国科学技术大学物理学院,
合肥 230026

刘朝星 助理教授

刘荧 教授
上海交通大学物理与天文系,
上海 200240

龙桂鲁 教授
清华大学物理系, 北京 100084

牛谦 教授

欧阳颀 教授, 院士
北京大学物理学院, 北京 100871

孙秀冬 教授
哈尔滨工业大学物理系, 哈尔滨 150001

童利民 教授
浙江大学光电信息工程学系,
杭州 310027

童彭尔 教授
香港科技大学物理系, 香港九龍

王开友 研究员
中国科学院半导体研究所, 北京 100083

魏苏淮 教授

解思深 研究员, 院士
中国科学院物理研究所, 北京 100190

叶朝辉 研究员, 院士
中国科学院武汉物理与数学研究所,
武汉 430071

郁明阳 教授

张富春 教授
香港大学物理系, 香港

张勇 教授

郑波 教授
浙江大学物理系, 杭州 310027

周兴江 研究员
中国科学院物理研究所, 北京 100190

Department of Physics, Sungkyunkwan University, Suwon, Korea

Physics Department, University of Wisconsin-Madison, Madison, USA

Prof. Cheng Jian-Chun
School of Physics, Nanjing University, Nanjing 210093, China

Prof. Dai Xi
Institute of Physics, Chinese Academy of Sciences, Beijing 100190, China

Prof. Academician Guo Guang-Can
School of Physical Sciences, University of Science and Technology of China, Hefei 230026, China

Assist. Prof. Liu Chao-Xing
Department of Physics, Pennsylvania State University, PA 16802-6300, USA

Prof. Liu Ying
Department of Physics and Astronomy, Shanghai Jiao Tong University, Shanghai 200240, China

Prof. Long Gui-Lu
Department of Physics, Tsinghua University, Beijing 100084, China

Prof. Niu Qian
Department of Physics, University of Texas, Austin, TX 78712, USA

Prof. Academician Ouyang Qi
School of Physics, Peking University, Beijing 100871, China

Prof. Sun Xiu-Dong
Department of Physics, Harbin Institute of Technology, Harbin 150001, China

Prof. Tong Li-Min
Department of Optical Engineering, Zhejiang University, Hangzhou 310027, China

Prof. Tong Peng'er
Department of Physics, The Hong Kong University of Science and Technology, Kowloon, Hong Kong, China

Prof. Wang Kai-You
Institute of Semiconductors, Chinese Academy of Sciences, Beijing 100083, China

Prof. Wei Su-Huai
National Renewable Energy Laboratory, Golden, Colorado 80401-3393, USA

Prof. Academician Xie Si-Shen
Institute of Physics, Chinese Academy of Sciences, Beijing 100190, China

Prof. Academician Ye Chao-Hui
Wuhan Institute of Physics and Mathematics, Chinese Academy of Sciences, Wuhan 430071, China

Prof. Yu Ming-Yang
Theoretical Physics I, Ruhr University, D-44780 Bochum, Germany

Prof. Zhang Fu-Chun
Department of Physics, The University of Hong Kong, Hong Kong, China

Prof. Zhang Yong
Electrical and Computer Engineering Department, The University of North Carolina at Charlotte, Charlotte, USA

Prof. Zheng Bo
Physics Department, Zhejiang University, Hangzhou 310027, China

Prof. Zhou Xing-Jiang
Institute of Physics, Chinese Academy of Sciences, Beijing 100190, China

编辑 Editorial Staff

王久丽 Wang Jiu-Li 章志英 Zhang Zhi-Ying 蔡建伟 Cai Jian-Wei 翟振 Zhai Zhen 郭红丽 Guo Hong-Li

Microscale vortex laser with controlled topological charge*

Xing-Yuan Wang(王兴远)¹, Hua-Zhou Chen(陈华洲)¹, Ying Li(黎颖)¹,
Bo Li(李波)¹, and Ren-Min Ma(马仁敏)^{1,2,†}

¹State Key Laboratory for Mesoscopic Physics and School of Physics, Peking University, Beijing 100871, China

²Collaborative Innovation Center of Quantum Matter, Beijing, China

(Received 20 October 2016; revised manuscript received 7 November 2016; published online 25 November 2016)

A microscale vortex laser is a new type of coherent light source with small footprint that can directly generate vector vortex beams. However, a microscale laser with controlled topological charge, which is crucial for virtually any of its application, is still unrevealed. Here we present a microscale vortex laser with controlled topological charge. The vortex laser eigenmode was synthesized in a metamaterial engineered non-Hermitian micro-ring cavity system at exceptional point. We also show that the vortex laser cavity can operate at exceptional point stably to lase under optical pumping. The microscale vortex laser with controlled topological charge can serve as a unique and general building block for next-generation photonic integrated circuits and coherent vortex beam sources. The method we used here can be employed to generate lasing eigenmode with other complex functionalities.

Keywords: exceptional point, non-Hermitian system, orbital angular momentum, vortex laser

PACS: 42.55.Px, 42.55.Sa, 42.60.By

DOI: 10.1088/1674-1056/25/12/124211

1. Introduction

Vortex beams are light beams with helical phase front possessing infinite topological charge and a phase singularity at the beam axis.^[1–3] These special properties inspired major interest for quantum information and communication, super-resolution imaging, micromanipulation, optical measurement, and digital imaging.^[4–14] The generation of optical vortex beam relies on the phase modulation of a laser beam either inside or outside of a laser cavity.^[1–3,15–29] To miniaturize the vortex beam generator, Cai *et al.* demonstrated an on-chip vortex emitter with well-defined orbital angular momentum by coupling light into a micro-ring with azimuthal scattering gratings.^[30] Recently, researches on metamaterial and exceptional point have provided a general method to manipulate electromagnetic field in a controlled manner.^[31–42] Miao *et al.* demonstrated a laser with emission carrying orbital angular momentum at microscale.^[43] However, a microscale laser with controlled topological charge, which is crucial for virtually any of its application, is still unrevealed.

Here we demonstrated a vortex laser with controlled topological charge at microscale. The vortex laser eigenmode synthesized in a micro-ring cavity at the exceptional point is stable enough to lasing state and emits vortex beam directly under optical pumping. Such a system can generate different orders of vortex beams by simply modulating the grating protruded on the micro-ring cavity. We obtained all these results from rigorous theoretical derivation and further proved them using three-dimensional (3D) full wave simulations.

2. Methods

2.1. Theoretical derivation

As for the vortex laser design, the key point is to construct an eigenmode in the microcavity which can emit vortex beam at desired order. First of all, we presented an analytical analysis for all kinds of exceptional points in a micro-ring cavity in the parameter space. Exceptional point is a singularity where both eigen-frequency and eigen-function coalesce. Here we employed a general form of refractive index modulation along the azimuthal direction of a micro-ring cavity and derived the conditions of exceptional point based on the coupled mode theory. Then, from the physical picture of scattering waves interference, we obtained the equations describing the parameters relationships of the refractive index modulations to achieve the exceptional point where only one propagating whispering-gallery mode exist at the lasing frequency. Secondly, a non-zero momentum perpendicular to the micro-ring plane is generated by introducing periodic gratings on the out wall of the micro-ring cavity. The out-of-plane momentum and the micro-ring cavity eigen-mode will twisted into an optical vortex beam. we can tune the order of the optical vortex emission by simply tuning the number of the grating elements along the outer sidewall.

2.2. Numerical simulation

The characteristics of the vortex laser is analyzed by 3D full wave simulations (Comsol Multiphysics). For a vortex

*Project supported by the “Youth 1000 Talent Plan” Fund, Ministry of Education of China (Grant No. 201421) and the National Natural Science Foundation of China (Grant Nos. 11574012 and 61521004).

†Corresponding author. E-mail: renminma@pku.edu.cn

laser cavity based on III–V InGaAsP gain materials as an example, the three dimensional eigen-mode solution will give all the information of the field distribution. The pumping effect of the cavity is treated as an increase of the imaginary part of InGaAsP refractive index. The stability of the vortex laser during the pumping is verified by the chirality of the angular momentum distribution in the lasing process. Q factor is calculated by the formula $Q = f_r/2f_i$, where f_r and f_i are the real and imaginary part of the eigenfrequency. Details for specific parameters can be found in the corresponding figure captions.

3. Results and discussion

3.1. Principles of a vortex laser

Figure 1 is the schematic diagram of a vortex laser. This vortex laser can generate arbitrary order of vortex beam. Here, we choose the second-order vortex beam as an example. Figure 1(a) presents the perspective view of the magnetic field $|H|$ distribution of a full wave simulation of the vortex laser on a log scale. Inside the laser cavity, the exceptional point ensures a unidirectional travelling whispering gallery mode, which is evidenced by the weak fluctuation of the magnetic field (Fig. 1(b)). Figure 1(c) shows the transversal distribution of the radial component of the magnetic field H_r in the far field, which presents a vortex beam profile. The vortex laser cavity is simulated with III–V InGaAsP gain materials, because its emission is at the C-band of the optical communication.^[44] The inner radius and the width of the vortex laser cavity are 1500 nm and 500 nm respectively.

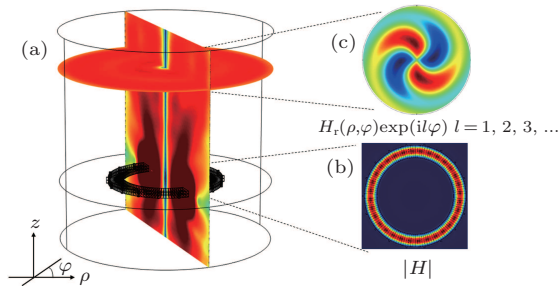


Fig. 1. (color online) Operation principles of a vortex laser. (a) A perspective view of the magnetic field $|H|$ distribution of a full wave simulated vortex laser on a log scale. (b) The exceptional point enables a unidirectional travelling whispering gallery mode inside the laser cavity evidenced by the weak fluctuation of magnetic field $|H|$. (c) The transversal distributions of radial component of the magnetic field H_r in the cross section of the vortex laser emission, showing typical optical vortex beam characteristic.

3.2. Exceptional points in the vortex laser cavity

The chirality mode at exceptional point is necessary for the realization of vortex laser with well-defined topological charge. Here we derived a general expression for the exceptional points in a vortex laser cavity. The derivation is based on the unsymmetrical coherent scattering between two degenerate counter propagating modes in a whispering-gallery micro-ring cavity. In a fundamental physical picture of interference, when the back scatterings from counter-clockwise (CCW) mode to clockwise (CW) mode interfere destructively

while the back scatterings from CW mode to CCW mode do not, the system locates at the exceptional point and degenerate eigen-modes of the system coalesce to a pure CCW traveling mode and *vice versa*.^[40] Here we employed two sets of periodic gratings to generate discrete momentums satisfying the resonance Bragg-scattering condition. Figure 2(a) shows a general form of the refractive index modulation along the azimuthal direction (φ):

$$n = \begin{cases} n_0 + \Delta_1 e^{i\phi_1}, & (l\pi/m \leq \varphi \leq l\pi/m + \delta\varphi_1), \\ n_0 + \Delta_2 e^{i\phi_2}, & (l\pi/m + \varphi_0 \leq \varphi \leq l\pi/m + \varphi_0 + \delta\varphi_2), \end{cases} \quad (1)$$

where $l = 0, 1, 2, \dots, 2m-1$. The micro-ring is divided into $2m$ periods. n_0 is the unperturbed part of the refractive index. The index modulation is given by complex number $\Delta_2 e^{i\phi_2}$ and $\Delta_1 e^{i\phi_1}$.

The two gratings, $\Delta n = \Delta_1 e^{i\phi_1}$ and $\Delta n = \Delta_2 e^{i\phi_2}$ can be viewed as two sources of scattering. The modulus of the effective refractive index modulation induced by each grating will modulate the amplitude of the corresponding backscattering while its position and the angular width of the effective refractive index modulation (ϕ_1 and ϕ_2) decides the relative phase of the corresponding back scattering. Based on the mode coupling theory, we can obtain all the possible grating configurations to achieve fully destructive interference in one direction with nondestructive interference in the other direction, *a.k.a.* the exceptional point in the vortex laser cavity.

Here, we show two special classes of exceptional points with simplified parameters: 1) $\delta\varphi_1 = \delta\varphi_2$, 2) $\phi_1 = 0$, and 3) $\phi_2 = \pi/2$, where parity time symmetry is included in both cases.

In case 1), where the two modulation parts have the same angular width $\delta\varphi_1 = \delta\varphi_2$, the refractive index modulation to realize exceptional points needs to satisfy the relations of $\Delta_1 = \Delta_2$ and $\phi_2 + 2m\varphi_0 - \phi_1 = \pi$. $\delta\varphi_1 = \delta\varphi_2$ and $\Delta_1 = \Delta_2$ ensure equal amplitudes of back scatterings. The initial phase difference of the two back scatterings is $\phi_2 - \phi_1$. The angular displacement φ_0 between the centers of the two gratings provides additional phase difference of $2m\varphi_0$. The two back scatterings interfere destructively when the total phase difference $\phi_2 + 2m\varphi_0 - \phi_1$ equals to π , leading to an exceptional point for the unidirectional traveling CCW mode.

Another class of refractive index modulation is case 2) $\phi_1 = 0$ and $\phi_2 = \pi/2$. Figures 2(b) and 2(c) show the relations the parameters need to satisfy. The systems with parameters locating at the parameter surface in Figs. 2(b) and 2(c) are at certain exceptional point. We can see that the PT-symmetrical refractive index modulation is only a special case ($2m\varphi_0 = \pi/2$, $2m\delta\varphi_1 = 2m\delta\varphi_2 = \pi$, and $\Delta_1 = \Delta_2$). To illustrate this, we solved the eigen-value problem under the condition of $\phi_1 = 0, \phi_2 = \pi/2, 2m\varphi_0 = \pi/2$. Figures 2(d) and 2(e) show the real part and imaginary part of the eigen-values respectively. Obviously, the systems corresponding to the clon-diagonal of the $n_R - n_I$ coordinate plate ($\Delta_1 = \Delta_2$) have coalesced eigen-value and thus locate at exceptional point.

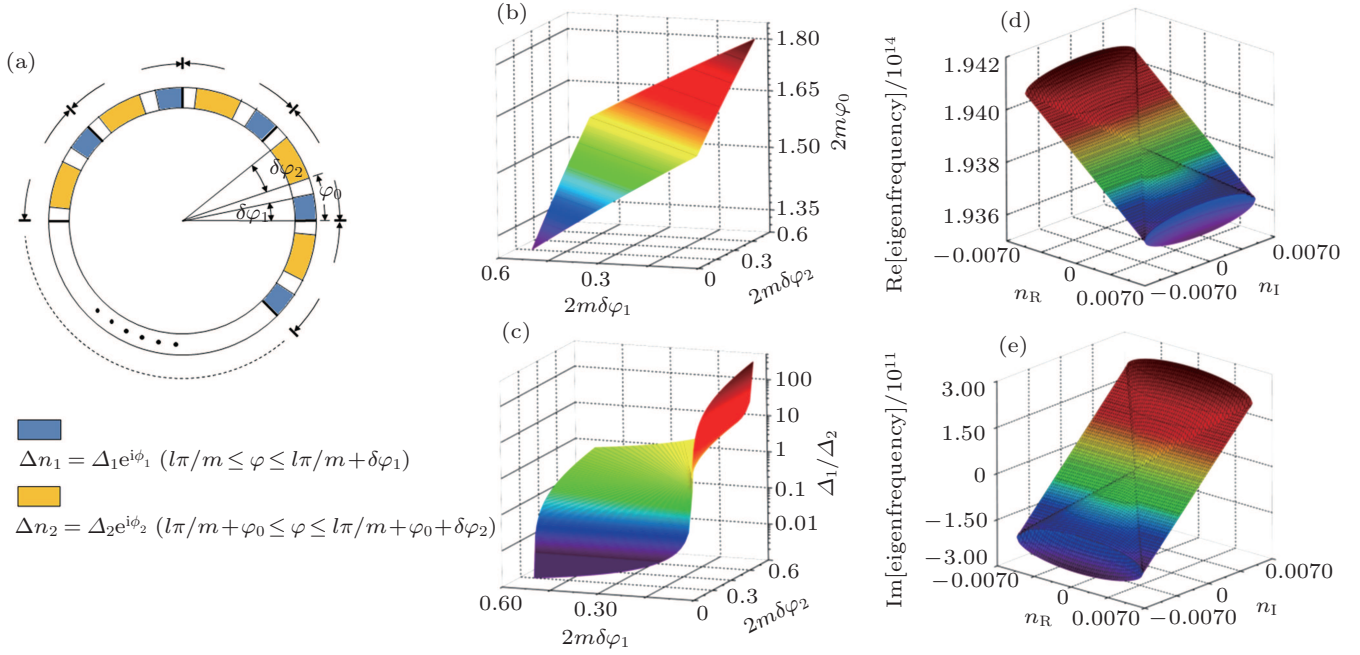


Fig. 2. (color online) Exceptional points in the vortex laser cavity. (a) A general form of refractive-index modulation in a micro-ring cavity. The index modulation consists of two sets of periodic scattering elements, which are essential to realize exceptional points in the view of interference. Panels (b) and (c) show the relations the parameters need to satisfy simultaneously to achieve exceptional points on the condition of $\phi_1 = 0$ and $\phi_2 = \pi/2$. Panels (d) and (e) are the real part and imaginary part of the eigen-values in the case of one grating with pure real part n_R ($n_R = \Delta_1 e^{i\phi_1}$, $\phi_1 = 0$) while the other grating with pure imaginary n_I ($n_I = \Delta_2 e^{i\phi_2}$, $\phi_2 = \pi/2$) index modulation and keeping $2m\varphi_0 = \pi/2$. This is the case of PT-symmetrical refractive index modulation. In the calculation, azimuthal order $m = 16$, refractive index of the cavity $n_0 = 2.67$, $\Delta n_R = n\pi/16 \leq \varphi \leq n\pi/16 + \pi/32$, $\Delta n_I = n\pi/16 + \pi/64 \leq \varphi \leq n\pi/16 + 3\pi/64$, $n = 0, 1, 2, \dots, 31$. The inner radius and the width of the vortex laser cavity is 1500 nm and 500 nm respectively.

3.3. Different orders of optical vortex generation on demand

Optical vortex with different orders of orbital angular momentum has an additional degree of freedom for multiplexing. Here, we presented the generation of optical vortex with different order while in the PT-symmetrical refractive index modulated system:

$$n = \begin{cases} n_0 + \Delta n_R, & (l\pi/m \leq \varphi \leq l\pi/m + \pi/4m), \\ n_0 + \Delta n_R + \Delta n_I i, & (l\pi/m + \pi/4m \leq \varphi \leq l\pi/m + \pi/2m), \\ n_0 + \Delta n_I i, & (l\pi/m + \pi/2m \leq \varphi \leq l\pi/m + 3\pi/4m), \end{cases} \quad (2)$$

where n_0 is the unperturbed part of the refractive index, and Δn_R and Δn_I are the real and imaginary index modulation, respectively. $l = 0, 1, 2, \dots, 2m-1$.

The $2m$ periods of refractive index modulation is chosen to tune the system to an exceptional point. At the same time the index modulation will not couple the beam into free space according to momentum-matching condition. This ensures that we can avoid uncontrollable additional orders of vortex beam. And then we choose the number of the outer sidewall grating q_{OWG} as $2m > q_{\text{OWG}} > m$. In this case, the outer sidewall grating does not cause the change of the exceptional point in parameter space. It only takes the role of coupling the travelling whispering-gallery mode and the free-space vortex beam mode. The order v_{rad} of the optical vortex is solely determined by the difference between azimuthal order m of the desired whispering gallery mode and the number of the outer

sidewall gratings:

$$v_{\text{rad}} = m - q_{\text{OWG}}. \quad (3)$$

The general results obtained are valid for both TE and TM polarized whispering-gallery modes. In our device with thin ring geometry, the effective index for TM modes is considerably decreased.^[45] Thus, the TE modes preferentially reach the lasing condition of the cavity. The magnetic field vector H_z of the TE modes are perpendicular to the cavity plane.

Vortex beams with arbitrary orbital angular momentum can be achieved by tuning the outer sidewall grating. Figure 3 shows that stable vortex beam with increasing orbital angular momentum can be obtained by changing q_{OWG} . As shown in Figs. 3(a), 3(e), and 3(i), almost homogeneous magnetic field intensity distributions on the ring can be obtained for generating different orders of optical vortex. The fluctuation of the corresponding field intensity distribution $|H|$ in the cross sec-

tion of the vortex beam is also very weak (Figs. 3(b), 3(f), and 3(j)). The transversal distributions of radial component H_r (Figs. 3(c), 3(g), and 3(k)) and the corresponding phase distributions $\arg(H_r)$ (Figs. 3(d), 3(h), and 3(l)) further confirm that the vortex beams emitted from cavities with outer sidewall

grating elements $q_{\text{OWG}} = 17, 18, 19$ have definite OAM $\hbar, 2\hbar,$ and $3\hbar$, respectively, which can be calculated from Eq. (3). These results are direct evidences indicating that the vortex laser can generate optical vortex with controllable definite orbital angular momentum.

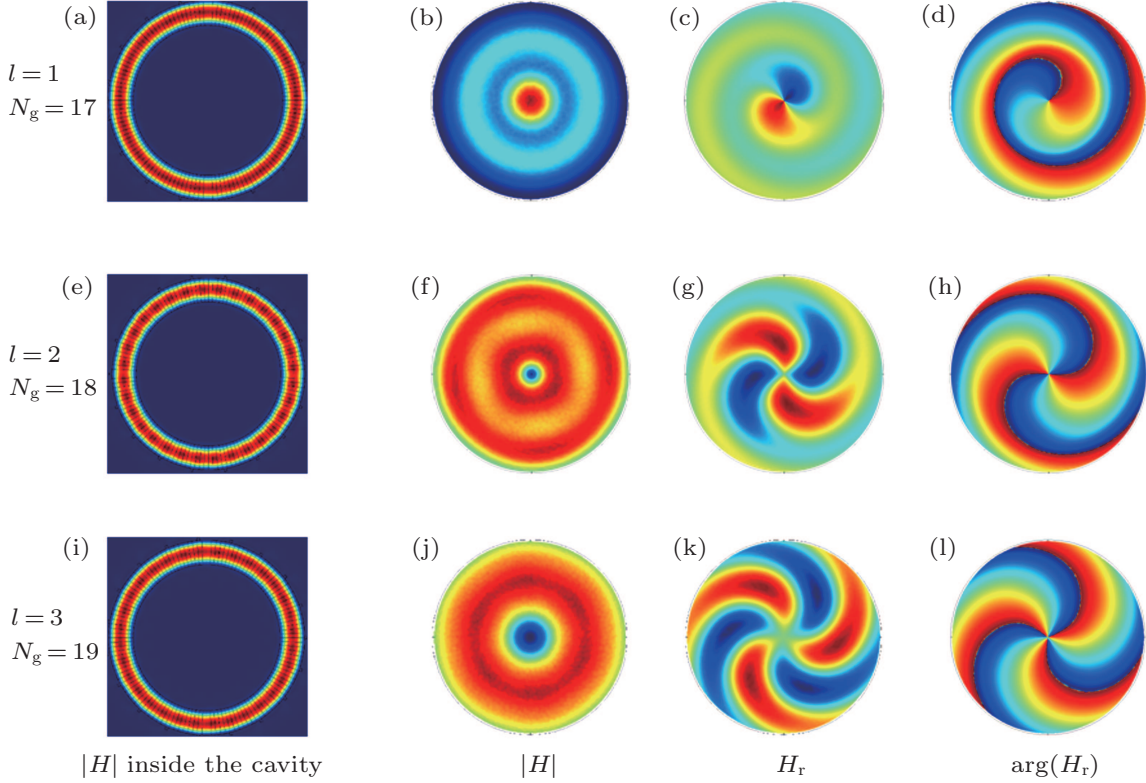


Fig. 3. (color online) Different orders of optical vortex generation on demand. (a)–(d) A Vortex laser with the first order of orbital angular momentum optical vortex emission, where the magnetic field intensity distributions inside the laser cavity (a), and $|H|$ (b), H_r (c), and $\arg(H_r)$ (d) at $4 \mu\text{m}$ above the lase cavity are depicted. (e)–(h) A Vortex laser with the second order of orbital angular momentum optical vortex emission, where the magnetic field intensity distributions inside the laser cavity (e), and $|H|$ (f), H_r (g), and $\arg(H_r)$ (h) at $4 \mu\text{m}$ above the lase cavity are depicted. (i)–(l) A Vortex laser with the third order of orbital angular momentum optical vortex emission, where the magnetic field intensity distributions inside the laser cavity (i), and $|H|$ (j), H_r (k), and $\arg(H_r)$ (l) at $4 \mu\text{m}$ above the lase cavity are depicted. All systems have the same index modulation ($\Delta n_r = \Delta n_t = 0.01$).

3.4. Visualization of vortex laser orbital angular momentum distribution

To further confirm the generation of the specific order of optical vortex, we decomposed the light field in the far field into a series of eigen-modes with different orbital angular momentum while the principle of the realization of vortex mode is also clearly shown. The field distribution can be decomposed by being expanded in cylindrical harmonics,^[45,46]

$$H_z(r, \varphi) = \sum_{m=-\infty}^{\infty} \alpha_m J_m(nkr) \exp(im\varphi), \quad (4)$$

where J_m is the m -th order Bessel function of the first kind, and k is the wave number, and n is the effective refractive index of the micro-ring. The CW (CCW) traveling-wave components are denoted by positive (negative) values of the angular momentum index m .^[46]

Figures 4(a) and 4(b) show the simulated intensity patterns $|H|$ and H_z in the far field of a vortex laser cavity

for generation of second order of orbital angular momentum emission. We can see that the fluctuation of the simulated magnetic pattern $|H|$ (Fig. 4(a)) is negligible at exceptional point. Figure 4(c) shows the ratio of the CW and CCW components $|\alpha_m|^2 / |\alpha_{-m}|^2$ as a function of real index modulation Δn_r with fixed $\Delta n_t = 0.01$. The exceptional point locates at $\Delta n_r = \Delta n_t$, at which the real and imaginary parts of the eigen-frequencies coalesce simultaneously. At $\Delta n_r = 0$, both eigenmodes have equal CW and CCW components ($|\alpha_{16}|^2 / |\alpha_{-16}|^2 \sim 1$) while in the vicinity of the exceptional point ($\Delta n_r = \Delta n_t$), both eigenmodes have dominant CCW component ($|\alpha_{16}|^2 / |\alpha_{-16}|^2 \gg 1$). These show an evolution from standing waves to traveling wave when the system is approaching the exceptional point. Especially, the simulation shows that the CCW component is about 484 times larger than the CW component at exceptional point, indicating a nearly perfect traveling wave mode.

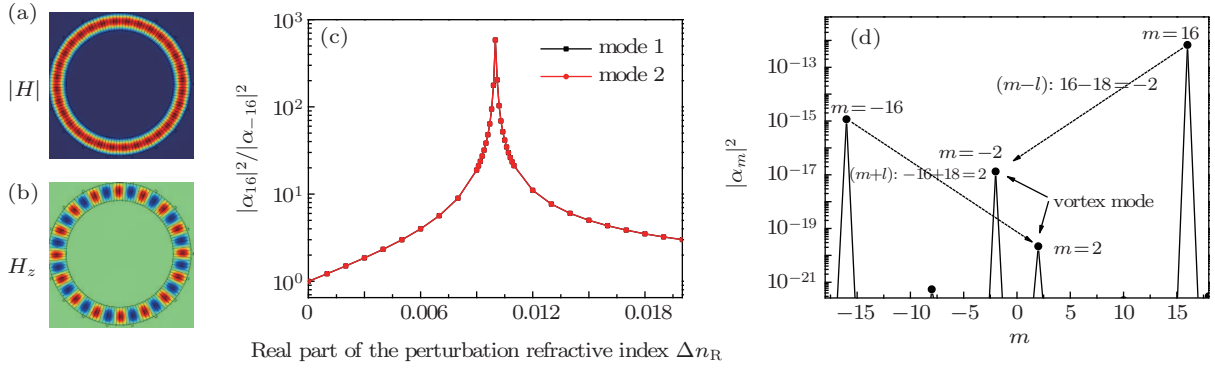


Fig. 4. (color online) Visualization of vortex laser angular momentum distribution. Panels (a) and (b) show the simulated intensity patterns $|H|$ and H_z of a mode inside the vortex laser cavity at $\Delta n_R = \Delta n_1$. The weak fluctuation of the $|H|$ and the periodicity of the H_z clearly show a 16-order traveling mode. (c) Ratio of CW and CCW component $|\alpha_m|^2/|\alpha_{-m}|^2$ as a function of real index modulation Δn_R . The imaginary index modulation is fixed at $\Delta n_1 = 0.01$. The mode shows clear chirality in the vicinity of the exceptional point ($\Delta n_R = \Delta n_1$). The CCW component is about 484 times larger than the CW component at exceptional point, which indicates a nearly perfect traveling wave mode. (d) Angular momentum distribution $|\alpha_m|^2$ of the whispering-gallery mode at exceptional point ($\Delta n_R = \Delta n_1 = 0.01$). The outer sidewall grating elements ($q_{\text{OWG}} = 18$) couple the dominated CW mode to the vertically emitted vortex beams with orbital angular momentum index $m = -2$ (16–18).

Figure 4(d) shows the orbital angular momentum distribution of the mode at exceptional point, which illustrates the physical process of the creation of the vortex beam. Under the index modulation, the CW modes are dominant (two orders larger than the CCW component while $m = 16$), and the outer sidewall grating elements ($q_{\text{OWG}} = 18$) couples CW and CCW traveling modes to the vertically emitting vortex beams with orbital angular momentum indexes $m = -2$ and $m = 2$, respectively. Thus, the emitted vortex beam with $m = -2$ from CW mode is two orders larger than the vortex beam with $m = 2$ from CCW mode, generating a vortex beam with definite angular momentum.

3.5. Stability of the vortex-beam output in the lasing process under pumping

Exceptional point is sensitive to the environmental parameters. Here we illustrate the stability of the vortex laser in the lasing process under uniform pumping. The uniform pumping of the gain material InGaAsP of the cavity is equivalent to increasing the imaginary part of refractive index n_1 of the InGaAsP. The uniformly changed background refractive index n_1 will only cause the change of the first order of the Fourier expansion coefficient of the refractive index, which will not induce additional coupling between the CCW and CW whispering-gallery modes according to the phase matching condition, and thus will not cause the change of the exceptional point in parameter space. We have confirmed this by 3D full wave simulations. As shown in Fig. 5(a), the vortex laser cavity mode becomes lasing and emitting vortex beam with the increase of n_1 . However, the ratio of orbital angular momentum components is almost unchanged as shown in Fig. 5(b), which confirms that the vortex laser is stable in the lasing process. The system is stable while $n_1 = -0.005$, corresponding to material gain of 202.5 cm^{-1} , which is achievable

in InGaAsP system.^[47]

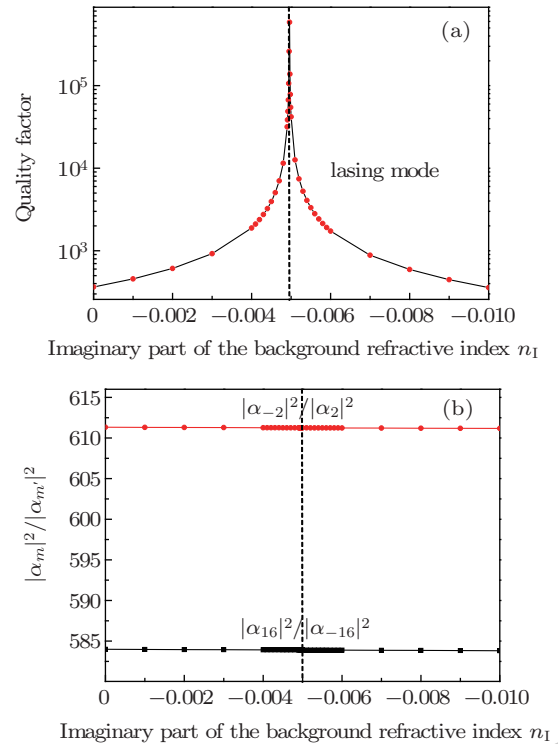


Fig. 5. (color online) Stability of the vortex-beam output in the lasing process under pumping. (a) The background gain dependence of the cavity quality factor for a vortex beam laser at exceptional point ($\Delta n_R = \Delta n_1 = 0.01$) with $N_g = 19$. The uniform pumping gain of the InGaAsP ring is mimicked by increasing the imaginary part of background refractive index n_1 . The quality factor is about 365 for the cavity without gain. With the increasing of the gain coefficient, the cavity quality factor increases by orders of magnitude, indicating that the loss is compensated by the gain. (b) Ratio of the CW and CCW components $|\alpha_m|^2/|\alpha_{-m}|^2$ as a function of background refractive index n_1 . The black dots show the main component of the mode is CW mode, which is almost unchanged with the increase of the background refractive index n_1 . The CW traveling mode is coupled to a vortex beam with azimuthal quantum number $m = -2$ (see the red dots).

4. Conclusions

In conclusion, the microscale vortex laser with controlled topological charge is demonstrated. The vortex laser eigen-

mode was synthesized in a meta-materials engineered non-Hermitian micro-ring cavity system and the optical vortex emission with defined orbital angular momentum can be obtained in a controlled manner. The vortex laser with controlled topological charge synergizes lasing and modulating functionalities in one device with microscale footprint, making it a unique and general building block for next-generation photonic integrated circuits and coherent vortex beam source.

References

- [1] Padgett M, Courtial J and Allen L 2004 *Phys. Today* **57** 35
- [2] Allen L, Beijersbergen M W, Spreeuw R and Woerdman J P 1992 *Phys. Rev. A* **45** 8185
- [3] Yao A M and Padgett M J 2011 *Adv. Opt. Photon.* **3** 161
- [4] Mair A, Vaziri A, Weihs G and Zeilinger A 2011 *Nature* **412** 313
- [5] Molina-Terriza G, Torres J P and Torner L 2007 *Nat. Phys.* **3** 305
- [6] Wang J, Yang J Y, Fazal I M, et al. 2012 *Nat. Photon.* **6** 488
- [7] Hui X N, Zheng S L, Chen Y L, et al. 2015 *Sci. Rep.* **5** 10148
- [8] Tamburini F, Anzolin G, Umbriaco G, Bianchini A and Barbieri C 2006 *Phys. Rev. Lett.* **97** 163903
- [9] He H, Heckenberg N R and Rubinszteindunlop H 1995 *J. Mod. Opt.* **42** 217
- [10] Friese M, Enger J, Rubinszteindunlop H and Heckenberg N R 1996 *Phys. Rev. A* **54** 1593
- [11] Toyoda K, Miyamoto K, Aoki N, Morita R and Omatsu T 2012 *Nano Lett.* **12** 3645
- [12] Zhou Z Y, Li Y, Ding D S, et al. 2014 *Opt. Lett.* **39** 5098
- [13] Fürhapter S, Jesacher A, Bernet S and Ritsch-Marte M 2005 *Opt. Lett.* **30** 1953
- [14] Torner L, Torres J P and Carrasco S 2005 *Opt. Express* **13** 873
- [15] Beijersbergen M W, Coerwinkel R, Kristensen M and Woerdman J P 1994 *Opt. Commun.* **112** 321
- [16] Li H L, Phillips D B, Wang X Y, et al. 2015 *Optica* **2** 547
- [17] Heckenberg N R, Mcduff R, Smith C P and White A G 1992 *Opt. Lett.* **17** 221
- [18] Marrucci L, Manzo C and Paparo D 2006 *Phys. Rev. Lett.* **96** 163905
- [19] Yu N F, Genevet P, Kats M A, et al. 2011 *Science* **334** 333
- [20] He J W, Wang X K, Hu D, et al. 2013 *Opt. Express* **21** 20230
- [21] Senatsky Y, Bisson JF, Li J, Shirakawa A, Thirugnanasambandam M and Ueda K I 2012 *Opt. Rev.* **19** 201
- [22] Oron R, Davidson N, Friesem A A, Hasman E and 2000 *Opt. Commun.* **182** 205
- [23] Oron R, Danziger Y, Davidson N, Friesem A A and Hasman E 1999 *Opt. Commun.* **169** 115
- [24] Bisson J F, Senatsky Y and Ueda K I 2005 *Laser Phys. Lett.* **7** 327
- [25] Itoh M and Yatagai T 2005 *Opt. Express* **15** 7616
- [26] Caley A J, Thomson M J, Liu J S, Waddie A J and Taghizadeh M R 2007 *Opt. Express* **15** 10699
- [27] Ito A, Kozawa Y and Sato S 2010 *J. Opt. Soc. Am. A* **27** 2072
- [28] Kano K, Kozawa Y and Sato S 2012 *Int. J. Opt.* **359** 141
- [29] Naidoo D, Roux F S, Dudley A, et al. 2016 *Nat. Photon.* **10** 327
- [30] Cai X L, Wang J W, Strain M J, et al. 2012 *Science* **338** 363
- [31] Heiss W D 2004 *J. Phys. A: Math. Gen.* **37** 2455
- [32] Wiersig J 2014 *Phys. Rev. A* **89** 012119
- [33] Lin Z, Ramezani H, Eichelkraut T, et al. 2011 *Phys. Rev. Lett.* **106** 213901
- [34] Peng B, Ozdemir S K, Rotter S, et al. 2016 *Proc. Natl. Acad. Sci.* **113** 6845
- [35] Liertzer M, Ge L, Cerjan A, et al. 2012 *Phys. Rev. Lett.* **108** 173901
- [36] Peng B, Ozdemir S K, Rotter S, et al. 2014 *Science* **346** 328
- [37] Dembowski C, Graf H D, Harney H L, et al. 2001 *Phys. Rev. Lett.* **86** 787
- [38] Heiss W D and Harney H L 2001 *Eur. Phys. J. D* **17** 149
- [39] Cao H and Wiersig J 2015 *Rev. Mod. Phys.* **87** 61
- [40] Zhu J G, Ozdemir S K, He L N and Yang L 2010 *Opt. Express* **18** 23535
- [41] Wiersig J 2014 *Phys. Rev. Lett.* **112** 203901
- [42] Wiersig J 2016 *Phys. Rev. A* **93** 033809
- [43] Miao P, Zhang Z, Sun J, et al. 2016 *Science* **353** 464
- [44] Killinger D 2002 *Opt. Photon. News* **13** 36
- [45] Frateschi N C and Levi A F J 1996 *J. Appl. Phys.* **80** 644
- [46] Wiersig J, Eberspacher A, Shim J B, et al. 2011 *Phys. Rev. A* **84** 023845
- [47] Leuthold J, Mayer M, Eckner J, Guekos G and Melchior H 2000 *J. Appl. Phys.* **87** 618

JUST FOR AUTHORS
— CHINESE PHYSICS B

Chinese Physics B

Volume 25

Number 12

December 2016

SPECIAL TOPIC — Acoustics

- 124301 Selective generation of ultrasonic Lamb waves by electromagnetic acoustic transducers**
Ming-Liang Li, Ming-Xi Deng and Guang-Jian Gao
- 124302 Improving the performance of acoustic invisibility with multilayer structure based on scattering analysis**
Chen Cai, Yin Yuan, Wei-Wei Kan, Jing Yang and Xin-Ye Zou
- 124303 Rayleigh reciprocity relations: Applications**
Ju Lin, Xiao-Lei Li and Ning Wang
- 124304 Quantitative damage imaging using Lamb wave diffraction tomography**
Hai-Yan Zhang, Min Ruan, Wen-Fa Zhu and Xiao-Dong Chai
- 124305 An acoustic bending waveguide designed by anisotropic density-near-zero metamaterial**
Yang-Yang Wang, Er-Liang Ding, Xiao-Zhou Liu and Xiu-Fen Gong
- 124306 A review of research progress in air-to-water sound transmission**
Zhao-Hui Peng and Ling-Shan Zhang
- 124307 Higher-order harmonics of general limited diffraction Bessel beams**
De-Sheng Ding and Jin-Huang Huang
- 124308 Nonlinear response of ultrasound contrast agent microbubbles: From fundamentals to applications**
Xu-Dong Teng, Xia-Sheng Guo, Juan Tu and Dong Zhang
- 124309 A three-dimensional coupled-mode model for the acoustic field in a two-dimensional waveguide with perfectly reflecting boundaries**
Wen-Yu Luo, Xiao-Lin Yu, Xue-Feng Yang, Ze-Zhong Zhang and Ren-He Zhang
- 124310 Spatial correlation of the high intensity zone in deep-water acoustic field**
Jun Li, Zheng-Lin Li and Yun Ren
- 124311 Bearing splitting and near-surface source ranging in the direct zone of deep water**
Jun-Nan Wu, Shi-Hong Zhou, Zhao-Hui Peng, Yan Zhang and Ren-He Zhang
- 124312 Research on the acoustic scattering function and coherence properties from rough seafloor based on finite element model**
Bo Lei, Yi-Xin Yang, Yuan-Liang Ma and Dong-Xu Chen
- 124313 Controls of pass-bands in asymmetric acoustic transmission**
Hong-Xiang Sun, Shu-Yi Zhang and Shou-Qi Yuan
- 124314 Ultrasound-mediated transdermal drug delivery of fluorescent nanoparticles and hyaluronic acid into porcine skin *in vitro***
Huan-Lei Wang, Peng-Fei Fan, Xia-Sheng Guo, Juan Tu, Yong Ma and Dong Zhang
- 124315 Developments of parabolic equation method in the period of 2000–2016**
Chuan-Xiu Xu, Jun Tang, Sheng-Chun Piao, Jia-Qi Liu and Shi-Zhao Zhang
- 124316 Generalized collar waves in acoustic logging while drilling**
Xiu-Ming Wang, Xiao He and Xiu-Mei Zhang

(Continued on the Bookbinding Inside Back Cover)

124317 Model/data comparison of typhoon-generated noise

Jing-Yan Wang and Feng-Hua Li

124318 Array gain for a conformal acoustic vector sensor array: An experimental study

Yong Wang, Yi-Xin Yang, Zheng-Yao He, Bo Lei, Chao Sun and Yuan-Liang Ma

RAPID COMMUNICATION

124211 Microscale vortex laser with controlled topological charge

Xing-Yuan Wang, Hua-Zhou Chen, Ying Li, Bo Li and Ren-Min Ma

125201 Filamentation instability in two counter-streaming laser plasmas

Hui Liu, Quan-Li Dong, Da-Wei Yuan, Xun Liu, Neng Hua, Zhan-Feng Qiao, Bao-Qiang Zhu, Jian-Qiang Zhu, Bo-Bin Jiang, Kai Du, Yong-Jian Tang, Gang Zhao, Xiao-Hui Yuan, Zheng-Ming Sheng and Jie Zhang

GENERAL

120201 Accurate reconstruction of the optical parameter distribution in participating medium based on the frequency-domain radiative transfer equation

Yao-Bin Qiao, Hong Qi, Fang-Zhou Zhao and Li-Ming Ruan

120301 New approach for anti-normally and normally ordering bosonic-operator functions in quantum optics

Shi-Min Xu, Yun-Hai Zhang, Xing-Lei Xu, Hong-Qi Li and Ji-Suo Wang

120302 Quantum process discrimination with information from environment

Yuan-Mei Wang, Jun-Gang Li, Jian Zou and Bao-Ming Xu

120303 Localization of quantum walks on finite graphs

Yang-Yi Hu and Ping-Xing Chen

120304 Controlled unknown quantum operations on hybrid systems

Yong He and Ming-Xing Luo

120305 Design of a gap tunable flux qubit with FastHenry

Naheed Akhtar, Yarui Zheng, Mudassar Nazir, Yulin Wu, Hui Deng, Dongning Zheng and Xiaobo Zhu

120401 Thermodynamics and geometrothermodynamics of regular black hole with nonlinear electrodynamics

Qiao-Shan Gan, Ju-Hua Chen and Yong-Jiu Wang

120601 Evaluation of the frequency instability limited by Dick effect in the microwave $^{199}\text{Hg}^+$ trapped-ion clock

Yi-He Chen, Lei She, Man Wang, Zhi-Hui Yang, Hao Liu and Jiao-Mei Li

120701 Synthesization of high-capacity auto-associative memories using complex-valued neural networks

Yu-Jiao Huang, Xiao-Yan Wang, Hai-Xia Long and Xu-Hua Yang

120702 Evidence of polymorphic transformations of Sn under high pressure

Qiu-Min Jing, Yu-Hong Cao, Yi Zhang, Shou-Rui Li, Qiang He, Qi-Yue Hou, Sheng-Gang Liu, Lei Liu, Yan Bi, Hua-Yun Geng and Qiang Wu

ATOMIC AND MOLECULAR PHYSICS

123101 Lattice structures and electronic properties of WZ-CuInS₂/WZ-CdS interface from first-principles calculations

Hong-Xia Liu, Fu-Ling Tang, Hong-Tao Xue, Yu Zhang, Yu-Wen Cheng and Yu-Dong Feng

123102 Dipole (hyper)polarizabilities of neutral silver clusters

Francisco E Jorge and Luiz G M de Macedo

123103 First-principle investigation on perovskite $\text{La}_{1-x}\text{Eu}_x\text{GaO}_3$

Yanni Gu, Sheng Xu and Xiaoshan Wu

123104 State-to-state quantum dynamics of $\text{N}(^2\text{D}) + \text{HD} (v = 0, j = 0)$ reaction

Yong Zhang

123601 Large adsorption energies for CO on Sc_n ($n = 2-8, 13$) nanoclusters

Jiang Meng

123701 Investigation of the thermal adaptability for a mobile cold atom gravimeter

Qi-Yu Wang, Zhao-Ying Wang, Zhi-Jie Fu and Qiang Lin

**ELECTROMAGNETISM, OPTICS, ACOUSTICS, HEAT TRANSFER, CLASSICAL MECHANICS,
AND FLUID DYNAMICS**

124201 Image transfer through coherent population trapping based on an atomic ensemble

Zhen-Hai Han and Dong-Sheng Ding

124202 Dynamics of two arbitrary qubits strongly coupled to a quantum oscillator

Kun Dong

124203 Flexible pulses from carbon nanotubes mode-locked fiber laser

Ling-ZhenYang, Yi Yang and Juan-Fen Wang

124204 Generation of femtosecond laser pulses at 396 nm in $\text{K}_3\text{B}_6\text{O}_{10}\text{Cl}$ crystal

Ning-Hua Zhang, Hao Teng, Hang-Dong Huang, Wen-Long Tian, Jiang-Feng Zhu, Hong-Ping Wu, Shi-Lie Pan, Shao-Bo Fang and Zhi-Yi Wei

124205 Spectra of spontaneous Raman scattering in taper-drawn micro/nano-fibers

Yingxin Xu, Liang Cui, Xiaoying Li, Cheng Guo, Yuhang Li, Zhongyang Xu, Lijun Wang and Wei Fang

124206 Cascade correlation-enhanced Raman scattering in atomic vapors

Hong-Mei Ma, Li-Qing Chen and Chun-Hua Yuan

124207 Nonlinear compression of picosecond chirped pulse from thin-disk amplifier system through a gas-filled hollow-core fiber

Jun Lu, Zhi-Yuan Huang, Ding Wang, Yi Xu, Yan-Qi Liu, Xiao-Yang Guo, Wen-Kai Li, Fen-Xiang Wu, Zheng-Zheng Liu and Yu-Xin Leng

124208 Modulation instabilities in randomly birefringent two-mode optical fibers

Jin-Hua Li, Hai-Dong Ren, Shi-Xin Pei, Zhao-Lou Cao and Feng-Lin Xian

124209 Crosstalk analysis of silicon-on-insulator nanowire-arrayed waveguide grating

Kai-Li Li, Jun-Ming An, Jia-Shun Zhang, Yue Wang, Liang-Liang Wang, Jian-Guang Li, Yuan-Da Wu, Xiao-Jie Yin and Xiong-Wei Hu

124210 Theoretical simulation of a polarization splitter based on dual-core soft glass PCF with micron-scale gold wire

Qiang Liu, Shuguang Li, Xinyu Wang and Min Shi

124401 A technique for simultaneously improving the product of cutoff frequency–breakdown voltage and thermal stability of SOI SiGe HBT

Qiang Fu, Wan-Rong Zhang, Dong-Yue Jin, Yan-Xiao Zhao and Xiao Wang

(Continued on the Bookbinding Inside Back Cover)

124501 Stability analysis of a simple rheonomic nonholonomic constrained system

Chang Liu, Shi-Xing Liu and Feng-Xing Mei

124601 Lubricant film flow and depletion characteristics at head/disk storage interface

Hong-Rui Ao, Zhi-Ying Han, Kai Zhang and Hong-Yuan Jiang

PHYSICS OF GASES, PLASMAS, AND ELECTRIC DISCHARGES

125202 A Ku-band magnetically insulated transmission line oscillator with overmoded slow-wave-structure

Tao Jiang, Jun-Tao He, Jian-De Zhang, Zhi-Qiang Li and Jun-Pu Ling

125203 Numerical simulation of a direct current glow discharge in atmospheric pressure helium

Zeng-Qian Yin, Yan Wang, Pan-Pan Zhang, Qi Zhang and Xue-Chen Li

CONDENSED MATTER: STRUCTURAL, MECHANICAL, AND THERMAL PROPERTIES

126101 Electro-optic response in thin smectic C* film with chevron structures

Aleksey A Kudreyko, Nail G Migranov and Dana N Migranova

126102 Tuning of magnetic properties of aluminium-doped strontium hexaferrite powders

Xiao-Mei Ma, Jie Liu, Sheng-Zhi Zhu and Hui-Gang Shi

126103 High-pressure structure and elastic properties of tantalum single crystal: First principles investigation

Jian-Bing Gu, Chen-Ju Wang, Wang-Xi Zhang, Bin Sun, Guo-Qun Liu, Dan-Dan Liu and Xiang-Dong Yang

126104 Room temperature direct-bandgap electroluminescence from a horizontal Ge ridge waveguide on Si

Chao He, Zhi Liu and Bu-Wen Cheng

126201 Strain-rate-induced bcc-to-hcp phase transformation of Fe nanowires

Hongxian Xie, Tao Yu, Wei Fang, Fuxing Yin and Dil Faraz Khan

126701 Landau damping in a dipolar Bose-Fermi mixture in the Bose-Einstein condensation (BEC) limit

S M Moniri, H Yavari and E Darsheshdar

CONDENSED MATTER: ELECTRONIC STRUCTURE, ELECTRICAL, MAGNETIC, AND OPTICAL PROPERTIES

127101 Electronic structure of O-doped SiGe calculated by DFT + U method

Zong-Yan Zhao, Wen Yang and Pei-Zhi Yang

127102 Band offsets engineering at $\text{Cd}_x\text{Zn}_{1-x}\text{S}/\text{Cu}_2\text{ZnSnS}_4$ heterointerface

Wujisiguleng Bao, Sachuronggui and Fang-Yuan Qiu

127103 Identification of surface oxygen vacancy-related phonon-plasmon coupling in TiO_2 single crystal

Jun-Hong Guo, Ting-Hui Li, Fang-Ren Hu and Li-Zhe Liu

127104 Large reversible magnetocaloric effect induced by metamagnetic transition in antiferromagnetic HoNiGa compound

Yi-Xu Wang, Hu Zhang, Mei-Ling Wu, Kun Tao, Ya-Wei Li, Tim Yan, Ke-Wen Long, Teng Long, Zheng Pang and Yi Long

127301 Effect of PECVD $\text{SiN}_x/\text{SiO}_y\text{N}_x$ -Si interface property on surface passivation of silicon wafer

Xiao-Jie Jia, Chun-Lan Zhou, Jun-Jie Zhu, Su Zhou and Wen-Jing Wang

- 127302 Hydrostatic pressure and temperature effects on the binding energy and optical absorption of a multi-layered quantum dot with a parabolic confinement**
Sami Ortakaya and Muharrem Kirak
- 127303 Coexistence of unipolar and bipolar modes in Ag/ZnO/Pt resistive switching memory with oxygen-vacancy and metal-Ag filaments**
Han-Lu Ma, Zhong-Qiang Wang, Hai-Yang Xu, Lei Zhang, Xiao-Ning Zhao, Man-Shu Han, Jian-Gang Ma and Yi-Chun Liu
- 127304 Ultralow turnoff loss dual-gate SOI LIGBT with trench gate barrier and carrier stored layer**
Yi-Tao He, Ming Qiao and Bo Zhang
- 127305 Analysis of the modulation mechanisms of the electric field and breakdown performance in AlGaN/GaN HEMT with a T-shaped field-plate**
Wei Mao, Ju-Sheng Fan, Ming Du, Jin-Feng Zhang, Xue-Feng Zheng, Chong Wang, Xiao-Hua Ma, Jin-Cheng Zhang and Yue Hao
- 127501 Tunable in-plane spin orientation in Fe/Si (557) film by step-induced competing magnetic anisotropies**
Jin Tang, Wei He, Yong-Sheng Zhang, Yan Li, Wei Zhang, Syed Sheraz Ahmad, Xiang-Qun Zhang and Zhao-Hua Cheng
- 127701 Investigations of thickness-shear mode elastic constant and damping of shunted piezoelectric materials with a coupling resonator**
Ji-Ying Hu, Zhao-Hui Li, Yang Sun and Qi-Hu Li
- INTERDISCIPLINARY PHYSICS AND RELATED AREAS OF SCIENCE AND TECHNOLOGY**
- 128101 Nanoscale spatial phase modulation of GaAs growth in V-grooved trenches on Si (001) substrate**
Shi-Yan Li, Xu-Liang Zhou, Xiang-Ting Kong, Meng-Ke Li, Jun-Ping Mi, Meng-Qi Wang and Jiao-Qing Pan
- 128102 Ultra-wideband circular-polarization converter with micro-split Jerusalem-cross metasurfaces**
Xi Gao, Xing-Yang Yu, Wei-Ping Cao, Yan-Nan Jiang and Xin-Hua Yu
- 128103 Hot corrosion behavior of the spray-formed nickel-based superalloy**
Min Xia, Tian-Fu Gu, Chong-Lin Jia and Chang-Chun Ge
- 128104 Influences of annealing on structural and compositional properties of Al₂O₃ thin films grown on 4H-SiC by atomic layer deposition**
Li-Xin Tian, Feng Zhang, Zhan-Wei Shen, Guo-Guo Yan, Xing-Fang Liu, Wan-Shun Zhao, Lei Wang, Guo-Sheng Sun and Yi-Ping Zeng
- 128201 Electrical and dielectric properties of Na_{1/2}La_{1/2}Cu₃Ti₄O₁₂ ceramics prepared by high energy ball-milling and conventional sintering**
H Mahfoz Kotb and Mohamad M Ahmad
- 128202 Can secondary nucleation exist in ice banding of freezing colloidal suspensions?**
Jia-Xue You, Jin-Cheng Wang, Li-Lin Wang, Zhi-Jun Wang, Jun-Jie Li and Xin Lin
- 128401 A high-power subterahertz surface wave oscillator with separated overmoded slow wave structures**
Guang-Qiang Wang, Jian-Guo Wang, Peng Zeng, Dong-Yang Wang and Shuang Li
- 128402 Modeling and experimental studies of a side band power re-injection locked magnetron**
Wen-Jun Ye, Yi Zhang, Ping Yuan, Hua-Cheng Zhu, Ka-Ma Huang and Yang Yang

(Continued on the Bookbinding Inside Back Cover)

- 128403 Cognitive radio adaptation for power consumption minimization using biogeography-based optimization**
Pei-Han Qi, Shi-Lian Zheng, Xiao-Niu Yang and Zhi-Jin Zhao
- 128501 Structure-dependent behaviors of diode-triggered silicon controlled rectifier under electrostatic discharge stress**
Li-Zhong Zhang, Yuan Wang and Yan-Dong He
- 128502 Bright hybrid white light-emitting quantum dot device with direct charge injection into quantum dot**
Jin Cao, Jing-Wei Xie, Xiang Wei, Jie Zhou, Chao-Ping Chen, Zi-Xing Wang and Chulgyu Jhun
- 128503 Low-bias negative differential conductance controlled by electrode separation**
Xiao-Hua Yi, Ran Liu, Jun-Jie Bi, Yang Jiao, Chuan-Kui Wang and Zong-Liang Li
- 128701 Cooperatively surrounding control for multiple Euler–Lagrange systems subjected to uncertain dynamics and input constraints**
Liang-Ming Chen, Yue-Yong Lv, Chuan-Jiang Li and Guang-Fu Ma
- 128702 The most common friend first immunization**
Fu-Zhong Nian and Cha-Sheng Hu
- 128703 Accuracy and effectiveness of self-gating signals in free-breathing three-dimensional cardiac cine magnetic resonance imaging**
Shuo Li, Lei Wang, Yan-Chun Zhu, Jie Yang, Yao-Qin Xie, Nan Fu, Yi Wang and Song Gao
- 128704 Modulation of intra- and inter-sheet interactions in short peptide self-assembly by acetonitrile in aqueous solution**
Li Deng, Yurong Zhao, Peng Zhou, Hai Xu and Yanting Wang
- 128901 Bottleneck effects on the bidirectional crowd dynamics**
Xiao-Xia Yang, Hai-Rong Dong, Xiu-Ming Yao and Xu-Bin Sun
- 128902 Synchronization investigation of the network group constituted by the nearest neighbor networks under inner and outer synchronous couplings**
Ting-Ting Li, Cheng-Ren Li, Chen Wang, Fang-Jun He, Guang-Ye Zhou, Jing-Chang Sun and Fei Han
- 128903 Epidemic spreading on random surfer networks with infected avoidance strategy**
Yun Feng, Li Ding, Yun-Han Huang and Zhi-Hong Guan
- 128904 An improved genetic algorithm with dynamic topology**
Kai-Quan Cai, Yan-Wu Tang, Xue-Jun Zhang and Xiang-Min Guan

JUST FOR AUTHORS
— CHINESE PHYSICS B